Research Article

Optimal Control of Anti-Angiogenesis and Radiation Treatments for Cancerous Tumor: Hybrid Indirect Solver

Iman Alimirzaei [ID] **and Alaeddin Malek** [ID]

Tarbiat Modares University, Tehran, Iran

Correspondence should be addressed to Alaeddin Malek; mala@modares.ac.ir

This paper proposes a real-life volume reduction for cancer cells using optimal doses of radiation and an anti-angiogenic drug. A generalized dynamical system based on the diffusion-consumption equation along with stimulation and inhibition factors is proposed. To achieve continuous and low-dose therapy, the related problem is simulated by an optimal regulator problem mathematically. By combining steepest descent, conjugate gradient, and Armijo techniques, a novel hybrid indirect iterative solver is designed. For accuracy and execution speed, the current solver is compared with an interior-point optimizer and sequential quadratic Hamiltonian methods. Cancer therapy under two different treatment strategies and 24 various versions of the general dynamical system is considered numerically. A comprehensive analysis of the corresponding outcomes is presented. Numerical results and related diagrams are provided.

1. Introduction

According to World Health Organization reports for the year 2019, cancer diseases are considered the main cause of death and the most important cause of life expectancy reduction [1]. Malek and Abbasi [2–5] in years 2016, 2019, 2020, and 2022 introduced some mathematical models to simulate and solve optimal control problems for cancer therapy. Cancer cells form and reproduce abnormal cells irregularly, while the proliferation of adult normal cells is based on the division and replacement of dying cells. General cancer therapies have two categories: treatments that directly kill cancer cells and treatments that prevent cancer cell growth. Cancer therapy usually has negative side effects. Thus, treatment is acceptable if there is a reasonable balance between the outcome and its negative side effects. Anti-angiogenic treatment is a cancer therapy to prevent cancer cell proliferation. Radiation therapy leads to direct cancer cell killing and is frequently combined with anti-angiogenic or other therapies to increase its effectiveness [6]. Several mathematical models have been proposed to describe the evolution of tumor anti-angiogenesis as

a dynamical system. Among them, the models developed by Hahnfeldt et al. [7] and Ergun et al. [8] are widely recognized as the most prominent. Hahnfeldt formulated a diffusion-consumption equation to model the concentration of stimulators and inhibitors both inside and outside the tumor. His research revealed that the inhibitor would have a significant impact on the target endothelial cells in the tumor, ultimately leading to growth proportional to the tumor surface, while the effect of stimulators would be relatively independent of tumor or vascular size. Endothelial cells play a significant role in carrying blood, nutrients, and oxygen to vital organs, while also facilitating the removal of deoxygenated blood from these organs [9]. In the Ergun model, the inhibition term is proportional to the tumor radius rather than its surface area, under the assumption that the system is in a steady state. Kienle et al. [10] considered an inconsistent convex combination of the Hahnfeldt (tumor surface) and Ergun (tumor radius) models; this combination would reduce the medical relevance. There are many studies that have separately used different dynamics of vascular carrying capacity. For example, Owolabi et al. [11] separately employed three different carrying capacity dynamics to

investigate the singular arc for the optimal problems. In this article, we generalize the Hahnfeldt model by aiming to provide an improved description of the vasculature's carrying capacity while incorporating optimal strategies in the existence of anti-angiogenesis and radiotherapy. Here, we face both mathematical and clinical challenges; regarding the clinical aspect, treatment strategies for tumor reduction are encountered during treatment and final time, where the final time is fixed. From a mathematical point of view, we consider the quadratic term to control doses in the objective function.

Numerical methods for solving optimal control problems fall into two main categories: indirect and direct approaches. In the indirect method, the calculus of variations determines the first-order optimality conditions for the optimal control problem [12–14]. This approach yields a multipoint boundary-value problem to find optimal solutions. In direct methods, the state and control variables of the optimal control problem are approximated in an appropriate manner, transforming the problem into nonlinear programming (NLP) [15, 16]. These two approaches stem from different philosophies. The indirect approach indirectly solves the problem (reason for naming indirect) by converting it into a boundary-value problem, solving a set of differential equations for the optimal solution. In contrast, the direct method transcribes an infinite-dimensional optimization problem into a finite-dimensional one, leading to the optimal solution. Iterative indirect methods, such as steepest descent, consist of two components. One part focuses on determining the direction of movement, while another part focuses on determining the length of the movement step required to reach the optimal solution [17, 18]. Hence, employing a hybrid indirect solver concept may be an appropriate approach.

Indirect methods utilize Pontryagin's maximum principle (PMP) to provide analytical insights into the optimal control problem, leading to a better understanding of the system's behavior. Moreover, indirect methods can yield highly accurate solutions when they converge. In contrast, while direct methods can handle a wide range of problems, the accuracy of their solutions depends on the discretization grid and initial guess [17, 19]. Furthermore, when dealing with NLP, we often find ourselves needing to employ black box software, with no access to its internal workings. Consequently, we are strongly motivated to adopt a hybrid indirect method for solving the optimal control problem, comprehensively analyzing the dynamical system under control. To achieve this, we prove the global convergence of the hybrid indirect solver.

This paper is organized as follows. In Section 2, we propose two different dynamical systems in the absence and presence of treatment with a novel generalized vasculature's carrying capacity. In Section 3, an optimal control therapy is presented that incorporates both anti-angiogenic and radiotherapy as two different control variables. Additionally, we propose a novel hybrid indirect method to solve the corresponding problem. Section 4 presents the numerical examples, while Section 5 discusses the results. Concluding remarks are provided in Section 6.

2. Problem Formulation

The simplified geometry for cancer treatment includes three types of cells: healthy cells, cancer cells, and endothelial cells. In this paper, a fact on the mathematical model is on the rate of nutrient consumption and the diffusion of nutrients and oxygen to various parts of the tumor and vascular blood vessels. More precisely, we focused on the interaction between cancer cells and endothelial cells. To describe their interaction, a 2-compartment, cell population-based model is employed. The model considers the cancer cell volume, denoted as p, and the endothelial cell volume, denoted as q, as variables. In the following subsections, we will discuss tumor dynamics, propose a general carrying capacity dynamics, and present its general dynamical systems in the absence and presence of treatments in full detail.

2.1. Tumor Dynamics. To describe tumor growth dynamics, there are three growth models: exponential growth, logistic growth, and Gompertzian growth [9]. In 1825, Benjamin Gompertz introduced and applied his growth and mortality law, which is often used to describe the growth of animals and plants, as well as the quantity or volume of bacteria and cancer cells over time [20]. The Gompertzian growth model offers several advantages compared to the exponential and growth models. Exponential and logistic growth models failed to accurately describe the experimental data, whereas the Gompertzian model exhibited remarkable descriptive capability [21]. Above all, the Gompertzian growth model effectively captures how tumor cells rely on nutrients, oxygen, and space in a continuous process. As the tumor grows, the availability of these essential resources gradually diminishes, causing the growth rate to slow down until the tumor reaches its maximum size [22]. Hence, we consider the Gompertzian growth model in the form of an ordinary differential equation (ODE):

$$\dot{p}(t) = -\xi p(t) \ln\left(\frac{p(t)}{q(t)}\right), \tag{1}$$

where ξ denotes the tumor growth parameter. Equation (1) implies that a tumor shrinks when $p(t)/q(t) > 1$. However, when $p(t)$ tends to zero, the Gompertzian growth model will suffer from singularity. Thus, the Gompertzian model is not an adequate description of very small tumor volumes [23]. Note that when tumor grows, we have $p(t)/q(t) < 1$ and in medical studies [24, 25], the Gompertzian growth model is responsible.

2.2. General Carrying Capacity Dynamics. The dynamical model for endothelial cells is represented by a balance equation between the stimulatory effect $S(p,q)$ and the inhibitory effect $I(p,q)$, given in the form:

$$\dot{q}(t) = S(p,q) - I(p,q). \tag{2}$$

Hahnfeldt proposed a diffusion-consumption equation with quasi-steady state to describe the concentration n of stimulators and inhibitors inside the tumor as

$$D^2 \nabla^2 n - cn + s_0 = 0, \qquad (3)$$

where D^2 is the diffusion coefficient, s_0 is the cells' secreting rate, and c is the cells' clearing rate. The diffusion-consumption equation (3) can be represented in both Cartesian and spherical coordinate systems as follows.

(i) In a Cartesian coordinate system, the inhibitor or stimulator concentration at the point (x, y, z) within the tumor at time t will be denoted as $n(x, y, z, t)$. The concentration n can be determined by solving the following differential equation:

$$D^2 \nabla^2 n(x, y, z, t) - cn(x, y, z, t) + s_0 = 0. \qquad (4)$$

(ii) In a spherical coordinate system $(\widehat{\rho}, \widehat{\theta}, \widehat{\varphi})$ [26], Hahnfeldt considered the concentration as an explicit function of the tumor radius, assuming a symmetric tumor for simplification. Consequently, the concentration n at a specific point within the tumor, located at a distance $\widehat{r}$ from the center, is introduced by solving the following differential equation:

$$n'' + \frac{2n'}{\widehat{r}} - \frac{cn}{D^2} + \frac{s_0}{D^2} = 0. \qquad (5)$$

After solving equation (5), Hahnfeldt determined the interior concentrations of the inhibitor $n_I(\widehat{r})$ and stimulator $n_S(\widehat{r})$ at a specific point within the tumor as follows:

$$\begin{cases} n_S(\widehat{r}, t) = \dfrac{s_0}{c}, \\[2mm] n_I(\widehat{r}, t) = \dfrac{s_0}{6D^2}\left(3\widehat{r}_0^2 - \widehat{r}^2\right), \end{cases} \qquad (6)$$

where $\widehat{r}_0$ represents the initial tumor radius. By considering equation (6), it is concluded that the inhibitor would have a significant impact on the target endothelial cells within the tumor, leading to growth proportional to the tumor surface or $(\text{volume})^{(2/3)}$. In contrast, the effect of stimulators would remain relatively independent of the tumor or vasculature size [7]. However, by utilizing integration in spherical coordinate system [26], we drive the total stimulation and inhibition concentration inside the tumor as follows:

$$S(\widehat{r}_0, t) = \int_0^{2\pi} \int_0^{\pi} \int_0^{\widehat{r}_0} n_S(\widehat{r}, t)\widehat{\rho}^2 \sin(\widehat{\varphi})d\widehat{\rho}d\widehat{\varphi}d\widehat{\theta} = \left(\frac{4\pi s_0}{3c}\right)\widehat{r}_0^3, \qquad (7)$$

$$I(\widehat{r}_0, t) = \int_0^{2\pi} \int_0^{\pi} \int_0^{\widehat{r}_0} n_I(\widehat{r}, t)\widehat{\rho}^2 \sin(\widehat{\varphi})d\widehat{\rho}d\widehat{\varphi}d\widehat{\theta} = \left(\frac{8\pi s_0}{15D^2}\right)\widehat{r}_0^5. \qquad (8)$$

Based on equation (7), we can conclude that the total stimulating effect is in accordance with either $\widehat{r}_0^3$ or $(\text{volume})^{(3/3)}$. Thus, the general form of the total stimulating effect can be proposed as follows:

$$S(p, q) = bp(t)^{\alpha_s} q(t)^{\beta_s}, \qquad (9)$$

where birth rate $b > 0$ and $\alpha_s + \beta_s = (3/3)$. Similarly, according to equation (8), the final expression of the total inhibition effect is in accordance with either $\widehat{r}_0^5$ or $(\text{volume})^{(5/3)}$. Thus, we can propose the general form for the total inhibition effect as

$$I(p, q) = dp(t)^{\alpha_i} q(t)^{\beta_i}, \qquad (10)$$

where $\alpha_i + \beta_i = (5/3)$ and death rate $d > 0$. Hahnfeldt made the assumption that the inhibition term prevents tumor cell production, which has an impact on endothelial cells. According to the total concentration of inhibition equation (8), there can also be other cases in which the inhibition term, in addition to preventing tumor cell production, also inhibits the endothelial cells production, thereby impacting endothelial cells once again. Thus, without losing generality, we propose the general carrying capacity dynamic as

$$\dot{q}(t) = bp(t)^{\alpha_s} q(t)^{\beta_s} - dp(t)^{\alpha_i} q(t)^{\beta_i}. \qquad (11)$$

From equation (11), we understand that working with only the tumor radius means working with the smallest geometrical dimension. Consequently, there are 4 choices for the stimulating effect and 6 choices for the inhibiting effect as follows:

$$\alpha_s, \beta_s \in \left\{0, \frac{1}{3}, \frac{2}{3}, \frac{3}{3}\right\} \quad \text{for } \alpha_s + \beta_s = \frac{3}{3}, \qquad (12)$$

$$\alpha_i, \beta_i \in \left\{0, \frac{1}{3}, \frac{2}{3}, \frac{3}{3}, \frac{4}{3}, \frac{5}{3}\right\} \quad \text{for } \alpha_i + \beta_i = \frac{5}{3}. \qquad (13)$$

According to the multiplication principle, the carrying capacity model can be written in 24 different ways, with each model being consistent with the actual tumor characteristics. For example, Hahnfeldt gives $\alpha_s = 1$, $\beta_s = 0$, $\alpha_i = (2/3)$, and $\beta_i = 1$ to write

$$\dot{q}(t) = bp(t) - dp(t)^{(2/3)} q(t). \qquad (14)$$

Ergun et al. [8] selected questionable values: $\alpha_s = 0$, $\beta_s = (2/3)$, $\alpha_i = 0$, and $\beta_i = (4/3)$, which are inconsistent with the actual tumor characteristics. The reason is that the inhibitor factor must be proportional to the tumor surface, while Ergun considered it to be proportional to the tumor radius (see equations (12) and (13)). Unfortunately, Kienle et al. [10], without providing any justification, made two mistakes: (i) using the above questionable values of the Ergun model and (ii) using an inconsistent convex combination of the Hahnfeldt model (proportional to tumor surface) and the Ergun model (proportional to tumor radius). From a mathematical point of view, with knowledge of the authors, the only possible selections for α_s, β_s, α_i, and β_i are the 24 cases given in this paper, and any selection except these 24 cases is questionable.

2.3. General Dynamical System in the Absence of Treatment.

Here, we propose and provide a description of the dynamical system under consideration in the absence of treatment for cancer cells and endothelial cells:

TABLE 1: Notation and numerical values for model parameters and state and control variables.

Symbol	Description	Unit	Value
Model parameters			
ξ	Tumor growth parameter	day^{-1}	0.084*
b	Tumor-induced stimulation parameter	day^{-1}	5.85*
d	Tumor-induced inhibition parameter	mm^{-2}day^{-1}	0.00873*
α	Tumor radiosensitivity parameter	Gy^{-1}	0.7**
β	Tumor radiosensitivity parameter	Gy^{-2}	0.14**
η	Endothelial radiosensitivity parameter	Gy^{-1}	0.136**
δ	Endothelial radiosensitivity parameter	Gy^{-2}	0.086**
γ	Anti-angiogenic elimination parameter	[kg/mg of dose]day^{-1}	0.15**
ρ	Tumor/endothelial repair rate	day^{-1}	$\ln(2)/0.02$**
State variables			
p	Primary tumor volume	mm^3	
p_0	Initial tumor volume	mm^3	8000
q	Carrying capacity of the vasculature	mm^3	
q_0	Initial carrying capacity of the vasculature	mm^3	11000
r	Variable associated with quadratic radiation effects		
r_0	Initial variable associated with quadratic radiation effects		0
Control variables			
u	Anti-angiogenic agent (AA) dose rate	[mg of dose/kg]	
w	Radiation agent (RA) dose rate	Gy	

References for * and ** are [7, 8]. The absorbed energy per unit mass of tissue is typically measured in units of gray (Gy).

$$
\begin{cases}
\dot{p}(t) = -\xi p(t) \ln\left(\dfrac{p(t)}{q(t)}\right), \\[2mm]
\dot{q}(t) = \mathrm{b}p(t)^{\alpha_s} q(t)^{\beta_s} - \mathrm{d}p(t)^{\alpha_i} q(t)^{\beta_i}, \\[2mm]
p(t_0) = p_0, \\[2mm]
q(t_0) = q_0,
\end{cases}
\tag{15}
$$

where $\alpha_s + \beta_s = (3/3)$ and $\alpha_i + \beta_i = (5/3)$. In the rest of this subsection, we discuss the existence and uniqueness solution for dynamical system (15).

2.3.1. Existence and Uniqueness Solution for General Dynamical System.

The purpose of this subsection is to establish the existence and uniqueness of the solution for the general dynamical system (15). To achieve this goal, we need to demonstrate measurability, locally Lipschitz, and locally integrable. Subsequently, we will apply the existence and uniqueness theorem as presented and proven by Sontag [27].

Lemma 1 (measurable). *Assume that dynamical system (15) is in the form $\dot{x}(t) = f(t, x(t))$ such that $f: I \times X \longrightarrow \mathbb{R}^2$, I is an interval from t_0 initial time to t_f final time, and $X = \{(p, q)|p, q \in \mathbb{R}^+\}$ is an open subset in $\mathbb{R}^2$. If the following properties hold, then for all values of α_s, β_s, α_i, and β_i that satisfy equations (12) and (13), $f(t, x(t))$ is measurable.*

(i) $f(., x): I \longrightarrow \mathbb{R}^2$ is measurable for each fixed x.

(ii) $f(t, .): X \longrightarrow \mathbb{R}^2$ is continuous for each fixed t.

Proof. (i) Consider an arbitrary set $x_1 = (p_1, q_1)$ in X and substitute in the dynamical system (15); we have vector function as follows:

$$
f(., x_1) = \begin{pmatrix} -\xi p_1 \ln\left(\dfrac{p_1}{q_1}\right) \\[3mm] \mathrm{b}p_1^{\alpha_s} q_1^{\beta_s} - \mathrm{d}p_1^{\alpha_i} q_1^{\beta_i} \end{pmatrix}.
\tag{16}
$$

We know that constant real-value functions are measurable. Thus, the vector function $f(., x)$ is measurable (see [26]; Section 3 Theorem 6). □

Proof. (ii) By substituting an arbitrary time $t_1 \in I$ in the dynamical system (15), the vector function $f(t_1, .)$ is similar to $f(., x_1)$. We know that constant real-value functions and their linear combinations are continuous. Thus, the vector function $f(t, .)$ is continuous. □

Lemma 2 (locally Lipschitz). *Suppose Lemma 1 holds. Then for all values of α_s, β_s, α_i, and β_i that satisfy equations (12) and (13), f is locally Lipschitz on X.*

Proof. To prove locally Lipschitz, we must show that there are for every $x_0 \in X$ a real number $\delta > 0$ and a locally integrable function $\alpha: I \longrightarrow \mathbb{R}^+$ such that

$$\forall x, y \in B_\delta(x_0), \quad \forall t \in I, \quad \|f(t,x) - f(t,y)\| \le \alpha \|x - y\|, \tag{17}$$

where $B_\delta(x_0)$ is a ball with radius δ and center x_0 contained in X. For this purpose, let $x := (p_1, q_1)$, $y := (p_2, q_2)$, and f_i be the ith element of vector function f for $i \in \{1, 2\}$. We have

$$\begin{aligned}
\|f_i(t,x) - f_i(t,y)\| &= \|f_i(t, (p_1, q_1)) - f_i(t, (p_2, q_2))\| \\
&= \|f_i(t, (p_1, q_1)) - f_i(t, (p_2, q_1)) + f_i(t, (p_2, q_1)) - f_i(t, (p_2, q_2))\| \\
&\le \|f_i(t, (p_1, q_1)) - f_i(t, (p_2, q_1))\| + \|f_i(t, (p_2, q_1)) - f_i(t, (p_2, q_2))\|.
\end{aligned} \tag{18}$$

According to the Lemma 1, vector function $f(t,.)$ is continuous and $B_\delta(x_0)$ is bounded and is not contained $(0, 0)$, so the following corresponding bounds can be considered. For $i = 1$, we have:

$$\begin{aligned}
\|f_1(t, (p_1, q_1)) - f_1(t, (p_2, q_1))\| &\le \xi \|(p_1 - p_2)\ln(q_1)\| + \xi \|p_2 \ln(p_2) - p_1 \ln(p_1)\| \le L_{1,p} \|p_1 - p_2\|, \\
\|f_1(t, (p_2, q_1)) - f_1(t, (p_2, q_2))\| &\le \xi \|p_2 \ln q_1 - p_2 \ln q_2\| \le L_{1,q} \|q_1 - q_2\|.
\end{aligned} \tag{19}$$

If the elements of x and y do not tend towards zero, then in this case, we can define $L_1' := \max\{L_{1,p}, L_{1,q}\}$, and similarly for $i = 2$, we have:

$$\begin{aligned}
\|f_2(t, (p_1, q_1)) - f_2(t, (p_2, q_1))\| &\le b \|q_1^{\beta_s}(p_2^{\alpha_s} - p_1^{\alpha_s})\| + d \|q_1^{\beta_i}(p_2^{\alpha_i} - p_1^{\alpha_i})\| \le L_{2,p} \|p_2 - p_1\|, \\
\|f_2(t, (p_2, q_1)) - f_2(t, (p_2, q_2))\| &\le b \|p_2^{\alpha_s}(q_2^{\beta_s} - q_1^{\beta_s})\| + d \|p_2^{\alpha_i}(q_2^{\alpha_i} - q_1^{\alpha_i})\| \le L_{2,q} \|q_2 - q_1\|.
\end{aligned} \tag{20}$$

Define $L_2' := \max\{L_{2,p}, L_{2,q}\}$ and $L' := \max\{L_1', L_2'\}$. By applying $(a + b \le 2\sqrt{a^2 + b^2})$, we have:

$$\|f_i(t,x) - f_i(t,y)\| \le L'\big(\|p_1 - p_2\| + \|q_1 - q_2\|\big) \le \sqrt{2}L' \|(p_1, q_1) - (p_2, q_2)\|. \tag{21}$$

Thus, f is locally Lipschitz. □

Lemma 3 (locally integrable). *Suppose Lemma 1 holds. Then f is locally integrable on t.*

Proof. To prove that f is locally integrable, we must show that the following inequality holds:

$$\forall x_0 \in X, \quad \exists \beta: I \longrightarrow \mathbb{R}^+, \forall t \in I, \|f(t, x_0)\| \le \beta(t), \tag{22}$$

where β is a locally integrable function. Consider an arbitrary set $x_0 = (p_0, q_0)$ in X and f_i as the ith element of vector function f for $i \in \{1, 2\}$; we define

$$\begin{aligned}
c_1 &:= -\xi p_0 \ln\left(\frac{p_0}{s_0}\right), \\
c_2 &:= b p_0^{\alpha_s} q_0^{\beta_s} - d p_0^{\alpha_i} q_0^{\beta_i},
\end{aligned} \tag{23}$$

and $C := \max\{c_1, c_2\}$. Thus, by introducing $\beta(t) = C + e^t$, the lemma is proved.

The presented Lemmas 1, 2, and 3 are the assumptions for Theorem 54 in [27], and by applying the aforementioned theorem, the existence and uniqueness of the solution for the general dynamical system (15) are concluded.

The following matters must be considered if one wants to use the proposed general dynamical system (15).

(i) *Scale.* The Hahnfeldt model is based on serious asymptotic analysis of the diffusion-consumption equation underlying tumor anti-angiogenesis and makes the reasonable assumption that the inhibitory factor in the dynamic is proportional to the tumor surface, while the Ergun model questionably scales down these to the tumor radius. The proposed general dynamical system (15) works with all the possible scaling features (see equations (12) and

(13)). However, the authors in Section 5 show that there are better selected values for α_s, β_s, α_i, and β_i compared with the Hahnfeldt model [7].

(ii) *Medical Relevance.* In the Hahnfeldt model and our proposed general dynamical system, the tumor-induced inhibition parameter d has $\mathrm{mm}^{-2}\mathrm{day}^{-1}$ dimension, while in the Ergun model, d has $\mathrm{mm}^{-1}\mathrm{day}^{-1}$ dimension. Indeed, it is not feasible to consider two different physical concepts for a given biological phenomenon when one is measured in terms of death rates per unit length and the other in terms of death rates per unit area. $\qquad\square$

2.4. General Dynamical System Modeling with Anti-Angiogenic Treatment.

The process of stimulating the formation of new blood vessels and capillaries in order to supply the tumor with the necessary nutrients is called tumor angiogenesis [11]. In contrast, anti-angiogenic treatment prevents the cancer cell nutrition by eradicating the current tumor blood vessels while restricting the formation of new blood vessels [28, 29]. Initially, it was assumed that anti-angiogenic therapy might not exhibit toxicity compared to other chemotherapeutic agents due to the genetic stability and quiescence of endothelial cells under normal physiological conditions, as well as the selectivity of targeted drugs. However, this assumption proved to be a miscalculation [30]. In Figure 1, it is shown that tumors initiate angiogenesis through the activation of vascular endothelial growth factor (VEGF). Over 60 anti-angiogenic agents (AAs) have existed in clinical trials in the US since 2006. For example, endostatin inhibits VEGF, disrupting the endothelial cell growth that forms the lining of the newly developed blood vessels [31–33].

We consider a control variable u that represents the AA dose and is taken as a Lebesgue-measurable function in a compact interval $[0, u_{\max}]$ with $u_{\max}$ denoting the highest dose. Thus, from equation (2), the dynamical model for endothelial cells volume under anti-angiogenic treatment yields [9]

$$\dot{q}(t) = S(p, q) - I(p, q) - \gamma q(t)u(t), \qquad (24)$$

where γ denotes the anti-angiogenic elimination parameter. Based on the above discussion and the proposed general dynamical system (15), the ODE system for anti-angiogenic treatment as monotherapy is given as follows:

$$\begin{cases} \dot{p}(t) = -\xi p(t)\ln\left(\dfrac{p(t)}{q(t)}\right), \\[2mm] \dot{q}(t) = \mathrm{b}p(t)^{\alpha_s}q(t)^{\beta_s} - \mathrm{d}p(t)^{\alpha_i}q(t)^{\beta_i} - \gamma q(t)u(t), \\[2mm] p(t_0) = p_0, \\[2mm] q(t_0) = q_0. \end{cases}$$

$$(25)$$

Numerous medical studies confirm that once monotherapy is halted, the tumor will grow back [34–36]. Thus, anti-angiogenic therapy is not efficient as a stand-alone treatment. Still, in combination with other therapies that destroy cancer cells, such as chemotherapy or radiotherapy, it can enhance their effect and lead to synergistic benefits [6, 8].

2.5. General Dynamical System Modeling with Radiotherapy.

For all types of tumors, radiotherapy is a common therapeutic approach. It is carried out in 60–70% of newly diagnosed cancer patients, either as monotherapy or as a combination treatment with surgery, chemotherapy, and anti-angiogenic therapy, which are useful [37, 38]. We consider a control variable w that represents the amount of the radiotherapy agent (RA) rate in a compact interval $[0, w_{\max}]$ with $w_{\max}$ denoting the highest dose rate. Wein, in the year 2000, modeled cancer cells radiation damage by [39]

$$-p(t)\left(\alpha + \beta\int_{t_0}^{t_f} w(s)\exp\left(-\rho(t-s)\right)\mathrm{d}s\right)w(t), \qquad (26)$$

where α and β are cancer cell radiosensitivity parameters, ρ is the tumor repair rate, and the final time t_f is fixed in every instance within this paper. Note that

$$r(t) := \int_{t_0}^{t_f} w(s)\exp\left(-\rho(t-s)\right)\mathrm{d}s, \qquad (27)$$

is the solution to the linear ODE given by

$$\begin{aligned} \dot{r}(t) &= -\rho\mathrm{r}(t) + w(t), \\ r(t_0) &= r_0. \end{aligned} \qquad (28)$$

Thus, the term that quantifies the radiation damage to the cancer cells can be written in the form

$$-p(t)(\alpha + \beta r(t))w(t). \qquad (29)$$

Notice that the radiation has a destructive effect on endothelial cells, so the damage to endothelial cells is given by

$$-q(t)(\eta + \delta r(t))w(t), \qquad (30)$$

where η and δ are endothelial cell radiosensitivity parameters. In the literature, often the effects of radiotherapy on healthy cells, cancer cells, and endothelial cells are modeled by a system of ODEs [40]. Based on the preceding discussion and the proposed general dynamical system (15), we write:

$$\begin{cases} \dot{p}(t) = -\xi p(t)\ln\left(\dfrac{p(t)}{q(t)}\right) - p(t)(\alpha + \beta r(t))w(t), \\[2mm] \dot{q}(t) = \mathrm{b}p(t)^{\alpha_s}q(t)^{\beta_s} - \mathrm{d}p(t)^{\alpha_i}q(t)^{\beta_i} - q(t)(\eta + \delta r(t))w(t), \\[2mm] \dot{r}(t) = -\rho\mathrm{r}(t) + w(t), \end{cases}$$

$$(31)$$

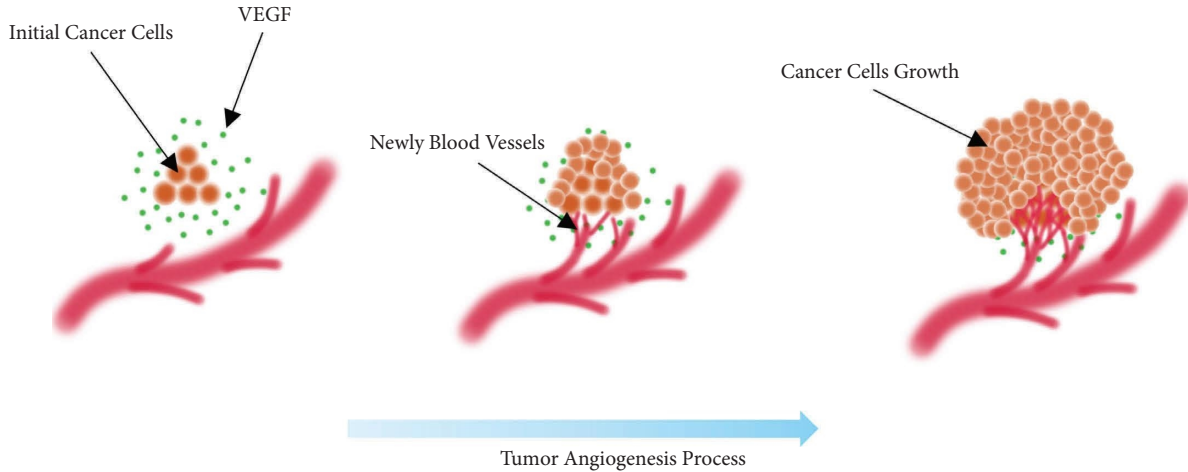with initial conditions $p(t_0) = p_0, q(t_0) = q_0$, and $r(t_0) = r_0$.

FIGURE 1: Angiogenic process and intense growth of cancer cells and endothelial cells.

2.6. General Dynamical System with Combined Therapy. The use of diversified methods in anti-cancer therapy offers a broader range of options for clinical treatment and enables the formation of robust partnerships [30]. For this purpose, the general dynamical system with control variables $u(t)$ and $w(t)$ for cancer therapy using the combination of anti-angiogenic treatment and radiotherapy is in the following form:

$$
\begin{cases}
\dot{p}(t) = -\xi p(t) \ln\left(\dfrac{p(t)}{q(t)}\right) - p(t)(\alpha + \beta r(t))w(t), \\[2ex]
\dot{q}(t) = \mathrm{b}p(t)^{\alpha_s} q(t)^{\beta_s} - \mathrm{d}p(t)^{\alpha_i} q(t)^{\beta_i} - q(t)(\eta + \delta r(t))w(t) - \gamma q(t)u(t), \\[2ex]
\dot{r}(t) = -\rho \mathrm{r}(t) + w(t), \\[2ex]
p(t_0) = p_0, \\[2ex]
q(t_0) = q_0, \\[2ex]
r(t_0) = r_0,
\end{cases}
\tag{32}
$$

where the parameter values and notation descriptions can be found in Table 1. The classification of the general dynamical system (32) using equations (12) and (13) leads to 24 distinct types of dynamical systems (see second column in Table 2).

3. Optimal Control Problem for a General Dynamical System

This paper aims to determine the optimal dosage scheme of AA and RA that minimizes tumor volume while causing the least harm to healthy cells. According to Food and Drug Administration recommendations and clinical discussions of the effectiveness of some AAs, it is reasonable to use the lowest possible dose [6, 41, 42]. On the other hand, in radiotherapy, the healthy cells around the cancer cells are almost destroyed, and the side effects depend on accuracy

and the amount of radiation dose [43]. Hence, the importance of optimal control methods in this context is significant.

3.1. Optimal Control Formulation. Based on the general dynamical system discussed in Section 2, one faces both mathematical and clinical challenges. Regarding the clinical aspect, treatment strategies for tumor reduction are encountered during treatment and the final time, where the final time is fixed. From a mathematical point of view, both linear and quadratic terms can be employed to control doses in the objective function. Numerous studies have demonstrated that administering continuous and low doses of therapeutic drugs leads to improved outcomes [44]. Ledzewicz et al. [45] investigated linear controls and determined

TABLE 2: Numerical results for 24 distinct versions of a general dynamical system for the optimal control problem (33), with a treatment strategy in Example 1.

No.	$(\alpha_s, \beta_s, \alpha_i, \beta_i)$	J^*	$p^*(t_f)$	$q^*(t_f)$	D_{AA}^*	D_{RA}^*
1	$(0, (3/3), 0, (5/3))$	4.020×10^3	86.847	1.233×10^4	70	10
2	$(0, (3/3), (1/3), (4/3))$	6.072×10^4	347.780	4.030×10^5	70	10
3	$(0, (3/3), (2/3), (3/3))$	4.119×10^8	2.870×10^4	2.171×10^7	70	0
4	$(0, (3/3), (3/3), (2/3))$	1.849×10^{15}	6.081×10^7	7.978×10^{22}	70	10
5	$(0, (3/3), (4/3), (1/3))$	5.835×10^{15}	1.080×10^8	2.419×10^{23}	70	10
6	$(0, (3/3), (5/3), 0)$	8.913×10^{15}	1.335×10^8	3.566×10^{23}	70	10
7	$((1/3), (2/3), 0, (5/3))$	958.633	40.232	1.296×10^3	52.90	10
8	$((1/3), (2/3), (1/3), (4/3))$	1.992×10^3	59.036	3.336×10^3	70	10
9	$((1/3), (2/3), (2/3), (3/3))$	6.004×10^3	107.289	1.236×10^4	69.75	10
10	$((1/3), (2/3), (3/3), (2/3))$	1.872×10^4	192.210	3.465×10^4	69.89	10
11	$((1/3), (2/3), (4/3), (1/3))$	3.433×10^4	261.085	5.580×10^4	70	10
12	$((1/3), (2/3), (5/3), 0)$	4.330×10^4	293.437	6.536×10^4	70	10
13	$((2/3), (1/3), 0, (5/3))$	463.763	27.760	428.625	35.198	10
14	$((2/3), (1/3), (1/3), (4/3))$	655.861	31.357	550.807	54.203	10
15	$((2/3), (1/3), (2/3), (3/3))$	921.419	37.294	700.984	66.085	10
16	$((2/3), (1/3), (3/3), (2/3))$	1.305×10^3	46.079	999.607	68.87	10
17	$((2/3), (1/3), (4/3), (1/3))$	1.782×10^3	55.422	1.244×10^3	69.37	10
18	$((2/3), (1/3), (5/3), 0)$	2.187×10^3	62.288	1.438×10^3	69.42	10
19	$((3/3), 0, 0, (5/3))$	297.917	22.309	240.407	26.400	10
20	$((3/3), 0, (1/3), (4/3))$	384.771	23.869	278.480	39.80	10
21	$((3/3), 0, (2/3), (3/3))$	478.261	25.171	301.336	52.998	10
22	$((3/3), 0, (3/3), (2/3))$	573.127	26.999	323.040	62.307	10
23	$((3/3), 0, (4/3), (1/3))$	665.911	29.396	344.896	66.762	10
24	$((3/3), 0, (5/3), 0)$	751.671	32.009	364.274	67.736	10

that optimal control is a singular arc, while bang-bang control fails to be optimal or desirable due to the need for dose continuity [12]. Therefore, we consider the quadratic term in the objective function to control doses, aiming to achieve continuous and low doses, as demonstrated in a previous study [12]. To ensure that the tumor volume remains nonnegative without introducing additional constraints, we express the tumor volume in a quadratic form within the objective function. The following optimal control problem (OCP) is considered as an optimal regulator problem [46]:

$$\text{OCP:} \begin{cases} \min_{(u,w)} J := \dfrac{\tau_p}{2} p(t_f)^2 + \dfrac{\theta_p}{2} \int_{t_0}^{t_f} p(t)^2 dt + \dfrac{\theta_u}{2} \int_{t_0}^{t_f} u(t)^2 dt + \dfrac{\theta_w}{2} \int_{t_0}^{t_f} w(t)^2 dt, \\[2mm] \text{subject to:} \\[2mm] \dot{p}(t) = -\xi p(t) \ln\left(\dfrac{p(t)}{q(t)}\right) - p(t)(\alpha + \beta r(t))w(t), \\[2mm] \dot{q}(t) = b p(t)^{\alpha_s} q(t)^{\beta_s} - d p(t)^{\alpha_i} q(t)^{\beta_i} - q(t)(\eta + \delta r(t))w(t) - \gamma q(t)u(t), \\[2mm] \dot{r}(t) = -\rho r(t) + w(t), \\[2mm] p(t_0) = p_0, \\[2mm] q(t_0) = q_0, \\[2mm] r(t_0) = r_0. \end{cases} \quad (33)$$

Here, according to control theory, $\mathscr{X} = (p, q, r)$ is a state space, and $\mathscr{U} = (u, w)$ is a control space.

3.2. Solving Optimal Control Problems: Direct and Indirect Methods.

There are two main numerical approaches to solve optimal control problems, depending on whether the problem is first optimized then discretized or vice versa. The purpose of the indirect method (optimize-then-discretize) is to find a solution to the ODE system resulting from Pontryagin's minimum principle. The direct method, a more recent approach, involves discretizing the optimal control problem and then finding the optimal solution to this discrete problem, which transforms into a finite-dimensional problem of nonlinear programming. Each of these two approaches has advantages and disadvantages [47, 48]. In recent years, numerous studies on cancer therapy with combinations of anti-angiogenic and radiotherapy treatments are done by direct methods. Using the direct method yields an NLP, which is solved by the interior-point optimizer (IPOPT) [49–52] via the Applied Mathematical Programming Language (AMPL) [53]. On the other hand, Kienle et al. [10] applied the sequential quadratic Hamiltonian (SQH) method as the indirect method, which was first introduced in [48, 54], to solve the related optimal control problem. Here, in this article, we propose a novel hybrid indirect method to solve the corresponding problem.

3.3. Optimality Conditions for the Optimal Control Problem.

We propose an optimization algorithm based on the indirect method for OCP (33). For this purpose, we apply the optimality necessary condition by using PMP. The general form for OCP (33) is as follows:

$$\min_{\mathscr{U} \in \mathscr{U}_{ad}} J = \phi\big(\mathscr{X}(t_f)\big) + \int_{t_0}^{t_f} L(\mathscr{X}(t), \mathscr{U}(t), t)\mathrm{d}t,$$

subject to

$$\dot{\mathscr{X}}(t) = f(\mathscr{X}(t), \mathscr{U}(t), t),$$

with initial conditions $\mathscr{X}(t_0) = (p_0, q_0, r_0)$,

$$(34)$$

where $\mathscr{U}_{ad}$ is admissible control space and is given by

$$\mathscr{U}_{ad} = \big\{(u, w) \in U \times W | U(t): [t_0, t_f] \longrightarrow [0, u_{\max}] \text{ and } W(t): [t_0, t_f] \longrightarrow [0, w_{\max}]\big\}. \tag{35}$$

We define the Hamiltonian function, which involves the integrand of the performance index and the costate variables with the right-hand side of the ODEs (34) in the form [48]

$$H = L(\mathscr{X}(t), \mathscr{U}(t), t) + \lambda^T f(\mathscr{X}(t), \mathscr{U}(t), t), \tag{36}$$

where λ represents the costate space. Specifically, the Hamiltonian function for OCP (33) is as follows:

$$H = \frac{\theta_p}{2}p^2 + \frac{\theta_u}{2}u^2 + \frac{\theta_w}{2}w^2 + \lambda_p\left(-\xi p \ln\left(\frac{p}{q}\right) - p(\alpha + \beta r)w\right)$$

$$+ \lambda_q\big(\mathrm{bp}^{\alpha_s}q^{\beta_s} - \mathrm{dp}^{\alpha_i}q^{\beta_i} - q(\eta + \delta r)w - \gamma\mathrm{qu}\big) + \lambda_r(-\rho\mathrm{r} + w), \tag{37}$$

where λ_p, λ_q, and λ_r are the corresponding costate variables for the state variables p, q, and r, respectively. Canonical Hamiltonian equations [46] for the OCP (33) using PMP yield

$$
\begin{cases}
\dot{\lambda}_p = -\theta_p p + \lambda_p \left(\xi \left(\ln \dfrac{p}{q} + 1 \right) + (\alpha + \beta r)w \right) + \lambda_q \left(d\alpha_i p^{\alpha_i - 1} q^{\beta_i} - b\alpha_s p^{\alpha_s - 1} q^{\beta_s} \right), \\[3mm]
\dot{\lambda}_q = -\lambda_p \xi \dfrac{p}{q} + \lambda_q \left(d\beta_i p^{\alpha_i} q^{\beta_i - 1} - b\beta_s p^{\alpha_s} q^{\beta_s - 1} + (\eta + \delta r)w + \gamma u \right), \\[3mm]
\dot{\lambda}_r = \lambda_p \beta p w + \lambda_q \delta q w + \lambda_r \rho, \\[3mm]
\dfrac{\partial H}{\partial u} = 0 \quad \text{thus,} \quad \theta_u u - \gamma \lambda_q q = 0, \\[3mm]
\dfrac{\partial H}{\partial w} = 0 \quad \text{thus,} \quad \theta_w w - \lambda_p (\alpha + \beta r)p - \lambda_q (\eta + \delta r)q + \lambda_r = 0, \\[3mm]
\text{with transversality conditions } \lambda_p(t_f) = \tau_p p(t_f), \lambda_q(t_f) = 0, \text{ and } \lambda_r(t_f) = 0.
\end{cases}
\tag{38}
$$

The general dynamical system (32) and canonical Hamiltonian equation (38) form a two-point boundary-value problem (TPBVP). If the boundary conditions are all given at either t_0 or t_f, one would numerically integrate the reduced differential equations to derive $\mathcal{X}^*(t)$ and $\lambda^*(t)$, $t \in [t_0, t_f]$ [48]. Unfortunately, the transversality conditions are dependent on state variables. Moreover, initial and transversality conditions are split, so the TPBVP cannot be solved in a standard manner [48]. Therefore, it is motivated to apply an iterative numerical technique to overcome these difficulties. By the hybrid technique here, we apply the steepest descent as an indirect method [48], conjugate gradient for search direction [55], and Armijo technique for the step length [56]. Although each of the three mentioned techniques exists in the literature, by integrating and implementing them, we have designed and developed a hybrid method to solve the optimal control problem. This hybrid method exhibits remarkable performance when compared to direct and indirect algorithms, which will be discussed in detail in the numerical results section.

3.4. Armijo Conjugate Steepest Descent Solver.

The steepest descent method is an iterative numerical technique used for determining the minimum of a differentiable function and is employed as an indirect method for solving the general dynamical system (32) and canonical Hamiltonian equation

(38). The main idea for solving them is to utilize the framework of the steepest descent method [48]. To search the direction, we use the conjugate gradient method as an exact line search [55]. Moreover, in order to determine distinct step lengths for the two control variables, we employ the Armijo technique [56] as an inexact line search method. The proposed hybrid method is called the Armijo conjugate steepest descent (ACSD) method. Here, the conjugate gradient direction is similar to the path opposite to ∇J with respect to the control variables u and w. For simplicity, in each step, the general dynamical system (32) and canonical Hamiltonian equation (38) are considered as the following form.

$$
\text{TPBVP:} \quad
\begin{cases}
\dot{\mathcal{X}}_i(t) = f\left(\mathcal{X}_i(t), \mathcal{U}_i(t), t \right), \\[3mm]
\dot{\lambda}_i(t) = -\dfrac{\partial \mathcal{H}}{\partial \mathcal{X}} \left(\mathcal{X}_i(t), \lambda_i(t), \mathcal{U}_i(t), t \right),
\end{cases}
\tag{39}
$$

and TPBVP (39) satisfies the boundary conditions

$$
\begin{aligned}
\mathcal{X}_i(t_0) &= (p(t_0), q(t_0), r(t_0)), \\
\lambda_i(t_f) &= (\tau_p p(t_f), 0, 0).
\end{aligned}
\tag{40}
$$

Nominal control history in each step will update by direction ψ_i and step length ϵ_i:

$$\mathcal{U}_{i+1}(t) = \mathcal{U}_i(t) + \epsilon_i \psi_i. \tag{41}$$

For better readability, in the following, we define $g_i := (\partial \mathcal{H}/\partial \mathcal{U})(\mathcal{X}_i(t), \lambda_i(t), \mathcal{U}_i(t), t)$. The value of ψ_i is determined through the conjugate gradient method using the following equation [55]:

$$\psi_i = \begin{cases} -g_i, & \text{if } i = 1, \\ -g_i + \zeta_i \psi_{i-1}, & \text{if } i \geq 2, \end{cases} \tag{42}$$

where ζ_i is a scalar in the following form:

$$\zeta_i = -\frac{g_i^T g_i}{\psi_{i-1}^T g_{i-1}}. \tag{43}$$

Furthermore, the computation of distinct step lengths $\epsilon_i = (\epsilon_{u_i}, \epsilon_{w_i})$ for the two control variables involves an inexact line search using the Armijo technique, as outlined in [44, 56]:

$$J(\mathcal{U}_i + \epsilon_i \psi_i) \leq J(\mathcal{U}_i) + \kappa \epsilon_i g_i^T \psi_i, \tag{44}$$

where $\kappa \in (0, 1)$ is known as Armijo backtracking parameter. Restrictions on AAs and RAs for nonnegativity and admissibility force us to put the following step to Algorithm 1.

$$\mathcal{U}_{i+1}(t) = \min\{\max\{0, \mathcal{U}_i(t) + \epsilon_i \psi_i\}, \mathcal{U}_{\max}\}, \tag{45}$$

where $\mathcal{U}_{\max} = (u_{\max}, w_{\max})$. Finally, the iteration is stopped when the criterion $\|\psi_i\| \leq \vartheta$ is satisfied, where ϑ is a preselected positive constant and we have:

$$\|\psi_i\|^2 = \int_{t_0}^{t_f} [\psi_i(t)]^T [\psi_i(t)] dt. \tag{46}$$

Hence, we summarize the Armijo steepest descent method for the general dynamical system (32) and canonical Hamiltonian equation (38) in Algorithm 1.

3.5. Convergence Analysis of the Armijo Conjugate Steepest Descent Method. In this subsection, we present the convergence analysis of the Armijo conjugate steepest descent method. For this purpose, we will demonstrate that the conjugate gradient coefficient satisfies a sufficient descent condition, and we will prove global convergence. Here, we define an additional condition by the Hamiltonian gradient and direction to ensure that the algorithm makes meaningful progress, as follows:

$$\exists \omega > 1, \quad \frac{\|g_{i+1}\|\|\psi_i\|}{\|\psi_i^T g_i\|} \leq 1 - \frac{1}{\omega}. \tag{47}$$

It is important to mention that equation (47) is more general than the curvature condition in the strong Wolfe conditions (see equation (3.7b) in [44]).

Lemma 4. *If we have Armijo conjugate steepest descent with conditions equations (44) and (47), then for $\|g_i\| \neq 0$, we have*

$$\|g_{i+1}\| - \|g_i\| < 0. \tag{48}$$

Proof. From equation (27) and the Cauchy–Schwarz properties, we have

$$\|g_{i+1}\|\|\psi_i\| \leq \left(1 - \frac{1}{\omega}\right)\|\psi_i^T g_i\| \leq \left(1 - \frac{1}{\omega}\right)\|\psi_i\|\|g_i\|. \tag{49}$$

Dividing both sides by $\|\psi_i\|$ yields

$$\|g_{i+1}\| - \|g_i\| \leq -\frac{1}{\omega}\|g_i\|. \tag{50}$$

The right-hand side of the above inequality is always negative. Thus, the proof is complete. $\square$

Lemma 5. *If we have Armijo conjugate steepest descent with conditions equations (44) and (47), then we have*

$$\frac{\|g_i\|}{\|\psi_i\|} \leq \frac{1}{1 - c}, \tag{51}$$

where $c \in (0, 1)$.

Proof. From equation (42), for $i = 1$, it is clear that $\|g_1\|/\|\psi_1\| = 1$, and for $i \geq 2$ by multiplying g_{i+1}^T, we have

$$g_{i+1}^T \psi_{i+1} = g_{i+1}^T (-g_{i+1} + \zeta_{i+1} \psi_i) = -\|g_{i+1}\|^2 + \zeta_{i+1} g_{i+1}^T \psi_i,$$

$$\|g_{i+1}\|^2 = -g_{i+1}^T \psi_{i+1} - g_{i+1}^T \frac{\|g_{i+1}\|^2}{\psi_i^T g_i} \psi_i. \tag{52}$$

Taking the absolute value and applying the Cauchy–Schwarz properties,

$$\|g_{i+1}\|^2 \leq \|g_{i+1}\|\|\psi_{i+1}\| + \|g_{i+1}\|\frac{\|g_{i+1}\|^2\|\psi_i\|}{\|\psi_i^T g_i\|}. \tag{53}$$

Therefore, we have

$$\|g_{i+1}\|^2 \left(1 - \frac{\|g_{i+1}\|\|\psi_i\|}{\|\psi_i^T g_i\|}\right) \leq \|g_{i+1}\|\|\psi_{i+1}\|, \tag{54}$$

and by dividing both sides of the above inequality by $\|g_{i+1}\|\|\psi_{i+1}\|$, we have

(1) Subdividing the interval $[t_0, t_f]$ into N equal subintervals and considering piecewise-constant controls:
    $\mathcal{U}_0(t) = \mathcal{U}_0(t_k), t_k \in [t_k, t_{k+1}), k = 0, 1, .., N-1$
(2) Applying the assumed control $\mathcal{U}_i$ to integrate the state equations from t_0 to t_f with initial condition $\mathcal{X}_i(t_0)$ and store the state matrix $\mathcal{X}_i$.
(3) Calculate $\lambda_i(t_f)$ from equation (40), use $\mathcal{U}_i$ and $\mathcal{X}_i$ to integrate the ODE costate from t_f to t_0, and store the costate matrix λ_i.
(4) Evaluate ψ_i from equation (42) and store as a vector.
(5) **if** $\|\psi_i\| \le \vartheta$ **then**
(6)   terminate the iterative procedure and output $\mathcal{U}_i$ and $\mathcal{X}_i$.
(7) **else**
(8)   find the ϵ_i from Armijo technique for the two control variables such that
       $J(\mathcal{U}_i + \epsilon_i \psi_i) \le J(\mathcal{U}_i) + \kappa \epsilon_i g_i^T \psi_i$.
(9)   adjust the piecewise-constant control by:
       $\mathcal{U}_{i+1}(t_k) = \min\{\max\{0, \mathcal{U}_i(t_k) + \epsilon_i \psi_i(t_k)\}, \mathcal{U}_{max}\}, k = 0, 1, \ldots, N-1,$
(10)   then replace $\mathcal{U}_i$ by $\mathcal{U}_{i+1}$ and return to step 2.
(11) **end if**

ALGORITHM 1: ACSD method.

$$\frac{\|g_{i+1}\|}{\|\psi_{i+1}\|}\left(1 - \frac{\|g_{i+1}\|\|\psi_i\|}{\|\psi_i^T g_i\|}\right) \le 1. \tag{55}$$

This suggests that

$$\frac{\|g_{i+1}\|}{\|\psi_{i+1}\|} \le \frac{1}{1 - (\|g_{i+1}\|\|\psi_i\|/\|\psi_i^T g_i\|)}. \tag{56}$$

From equation (47),

$$\frac{\|g_{i+1}\|}{\|\psi_{i+1}\|} \le \omega \text{ or } \|g_{i+1}\| \le \omega \|\psi_{i+1}\|. \tag{57}$$

Thus, the proof is complete.   □

Theorem 6. *Assuming that ψ_i is generated using equation (42) and ζ_i is obtained from equation (43), a sufficient condition is satisfied when*

$$g_i^T \psi_i \le -M \|g_i\|^2, \tag{58}$$

where $M > 0$ holds.

Proof. Multiplying both sides of equation (42) by g_{i+1}^T and using ζ_{i+1} yields

$$g_{i+1}^T \psi_{i+1} = g_{i+1}^T(-g_{i+1} + \zeta_{i+1}\psi_i)$$
$$= -\|g_{i+1}\|^2 - \frac{\|g_{i+1}\|^2}{\psi_i^T g_i} g_{i+1}^T \psi_i, \tag{59}$$

and we have

$$g_{i+1}^T \psi_{i+1} + \|g_{i+1}\|^2 = -\frac{\|g_{i+1}\|^2}{\psi_i^T g_i} g_{i+1}^T \psi_i. \tag{60}$$

For the right-hand side of the above inequality, we can take the absolute value and apply the Cauchy–Schwarz properties:

$$g_{i+1}^T \psi_{i+1} + \|g_{i+1}\|^2 \le \frac{\|g_{i+1}\|^2}{\psi_i^T g_i} \|g_{i+1}^T\| \|\psi_i\|. \tag{61}$$

By employing the condition stated in equation (47), we obtain:

$$g_{i+1}^T \psi_{i+1} \le \|g_{i+1}\|^2 \left(-1 + 1 - \frac{1}{\omega}\right). \tag{62}$$

The proof is complete. Therefore, for $\|g_{i+1}\| \ne 0$, this implies that

$$g_{i+1}^T \psi_{i+1} < 0. \tag{63}$$

The following theorem provides proof of the Zoutendijk conditions [57], establishing the global convergence of Armijo conjugate steepest descent with the new condition (47).   □

Theorem 7. *Consider the Armijo conjugate steepest descent method, where ϵ_i is obtained using the Armijo inexact line search rule equations (44) and (47). Assuming Lemma 4, Lemma 5, and Theorem 6 hold true, then either*

$$\lim_{i \to \infty} \|g_i\| = 0 \text{ or } \sum_{i=1}^{\infty} \frac{(g_i^T \psi_i)^2}{\|\psi_i\|^2} < \infty. \tag{64}$$

Proof. We employ a proof by contradiction argument. If Theorem 7 is not true, then there exists $a > 0$, such that

$$\|g_i\| \ge a. \tag{65}$$

From equation (42),

$$\psi_{i+1} + g_{i+1} = \zeta_{i+1}\psi_i. \tag{66}$$

Upon squaring both sides of the above equation, we have

$$\|\psi_{i+1}\|^2 = \zeta_{i+1}^2 \|\psi_i\|^2 - 2g_{i+1}^T \psi_{i+1} - \|g_{i+1}\|^2. \qquad (67)$$

Dividing both sides by $(g_{i+1}^T \psi_{i+1})^2$ yields

$$\frac{\|\psi_{i+1}\|^2}{(g_{i+1}^T \psi_{i+1})^2} = \frac{(\zeta_{i+1})^2 \|\psi_i\|^2}{(g_{i+1}^T \psi_{i+1})^2} - \frac{2}{g_{i+1}^T \psi_{i+1}} - \frac{\|g_{i+1}\|^2}{(g_{i+1}^T \psi_{i+1})^2}$$

$$= \frac{(\zeta_{i+1})^2 \|\psi_i\|^2}{(g_{i+1}^T \psi_{i+1})^2} - \left(\frac{1}{\|g_{i+1}\|} + \frac{\|g_{i+1}\|}{g_{i+1}^T \psi_{i+1}} \right)^2 + \frac{1}{\|g_{i+1}\|^2} \qquad (68)$$

$$\leq \frac{(\zeta_{i+1})^2 \|\psi_i\|^2}{(g_{i+1}^T \psi_{i+1})^2} + \frac{1}{\|g_{i+1}\|^2}.$$

Applying equation (43) yields

$$\frac{\|\psi_{i+1}\|^2}{(g_{i+1}^T \psi_{i+1})^2} \leq \left(\frac{\|g_{i+1}\|^2}{\|\psi_i\| \|g_i\|} \right)^2 \frac{\|\psi_i\|^2}{(g_{i+1}^T \psi_{i+1})^2} + \frac{1}{\|g_{i+1}\|^2} = \frac{\|g_{i+1}\|^2}{\|g_i\|^2 \|\psi_{i+1}\|^2} + \frac{1}{\|g_{i+1}\|^2}$$

$$\leq \frac{\|g_{i+1}\|^2}{\omega^2 \|\psi_i\|^2 \|\psi_{i+1}\|^2} + \frac{1}{\|g_{i+1}\|^2} \leq \frac{1}{\|\psi_i\|^2} + \frac{1}{\|g_{i+1}\|^2}. \qquad (69)$$

From equation (57) of Lemma 5, we have

$$\frac{\|\psi_{i+1}\|^2}{(g_{i+1}^T \psi_{i+1})^2} \leq \frac{\omega^2}{\|g_i\|^2} + \frac{1}{\|g_{i+1}\|^2}, \qquad (70)$$

and based on equation (48) of Lemma 4, we have

$$\frac{\|\psi_{i+1}\|^2}{(g_{i+1}^T \psi_{i+1})^2} < \frac{\omega^2 + 1}{\|g_{i+1}\|^2}. \qquad (71)$$

On the other hand, from equation (59), we have:

$$g_{i+1}^T \psi_{i+1} = -\|g_{i+1}\|^2 - \frac{\|g_{i+1}\|^2}{\psi_i^T g_i} g_{i+1}^T \psi_i. \qquad (72)$$

For the right-hand side of the above inequality, we can take the absolute value and apply the Cauchy–Schwarz properties:

$$g_{i+1}^T \psi_{i+1} \leq \|g_{i+1}\|^2 + \frac{\|g_{i+1}\|^2}{\|\psi_i^T g_i\|} \|g_{i+1}\| \|\psi_i\|. \qquad (73)$$

By employing the condition stated in equation (47), we obtain:

$$g_{i+1}^T \psi_{i+1} \leq \|g_{i+1}\|^2 \left(2 - \frac{1}{\omega} \right). \qquad (74)$$

We know that $(2 - 1/\omega) > 1$, and thus

$$\|g_{i+1}\|^2 \geq \frac{(g_{i+1}^T \psi_{i+1})}{(2 - (1/\omega))}. \qquad (75)$$

Substitute equation (75) in equation (71), and we get

$$\left(2 - \frac{1}{\omega} \right) (g_{i+1}^T \psi_{i+1}) > \frac{\|\psi_{i+1}\|^2}{\omega^2 + 1}. \qquad (76)$$

Dividing both sides by $(2 - (1/\omega))$ yields

$$(g_{i+1}^T \psi_{i+1}) > \frac{\|\psi_{i+1}\|^2}{(2 - (1/\omega))(\omega^2 + 1)}. \qquad (77)$$

By applying equation (57), we have

$$(g_{i+1}^T \psi_{i+1}) > \frac{\|g_{i+1}\|^2}{\omega^2 (2 - (1/\omega))(\omega^2 + 1)}$$

$$\geq \frac{a^2}{\omega^2 (2 - (1/\omega))(\omega^2 + 1)}. \qquad (78)$$

The right-hand side of the above inequality is always positive; then

$$(g_{i+1}^T \psi_{i+1}) > 0. \qquad (79)$$

This contradicts equation (63) in Theorem 6. Therefore, the proof is completed.

The questions to be asked at this stage are these:

(i) Can we determine values for α_s, β_s, α_i, and β_i from the values of second column in Table 2 so that they satisfy OCP (33)?

(ii) Do indirect methods work better compared to direct methods?

(iii) Between the ACSD and SQH solvers, which one is better?

(iv) What are the effects of tumor and carrying capacity volumes on inhibition and stimulation factors?

(v) Which one of the treatment strategies makes more medical sense?   □

4. Numerical Examples

In this section, we present the raw data obtained from three different methods: ACSD (Algorithm 1), IPOPT-AMPL, and SQH, used to solve the optimal control problem (33), considering 24 distinct versions of a general dynamical system and two treatment strategies. Comparisons are performed for the cost, cancer cell volume, endothelial cell volume, elapsed CPU time, total AA doses (computed as L_1-integrals) denoted as D_{AA}, and total RA doses (computed as L_1-integrals) denoted as D_{RA} utilized in the treatment. Goedegebuure et al. [58] confirmed that fractionated low-dose radiotherapy, i.e., daily fractions of up to 2 Gy, has a positive effect on cancer cells. Thus, in the following two different examples, we bound the w_{max} to be less than or equal to 2 Gy. The results have been conducted on an Intel Core i5 CPU 6th Generation at 2.4 GHz, with 4 GB RAM.

Example 1. This example aims to solve and analyze 24 distinct versions of a general dynamical system for the optimal control problem (33), with a treatment strategy to reduce tumor volume at the final time as optimal regulator problem in Bolza form. The admissible control space $(u, w) \in [0, 7] \times [0, 1]$ is considered, while the parameter values are given by $t_f = 10$, $\tau_p = 1$, $\theta_p = 0$, $\theta_u = 1$, $\theta_w = 1$, and others in Table 1. Our proposed Armijo conjugate steepest descent method is used as the solver, and the results are reported in Table 2. Note that dynamical system number 21 in Table 2 is known as the Hahnfeldt dynamical system.

Figure 2 depicts the comparison among the four selected dynamical systems in Example 1, including tumor volume, vascular carrying capacity, and the amounts of anti-angiogenic and radiation agents. In Figure 2(b), the optimal vascular carrying capacity of dynamical system 21 initially increased slightly and then decreased. The reason for this event is the role of vascular carrying capacity in the inhibiting factor. Strictly speaking, by reducing the effect of vascular carrying capacity, the response to anti-angiogenic treatment also decreases. In Figure 2(c), considering the daily dosage limit for the anti-angiogenic drug, dynamical system 21 exhibited the highest consumption of the drug between days 5 and 8. However, its performance in terms of the final tumor volume was not as effective. In contrast, dynamical system 19 had lower anti-angiogenic drug usage throughout the treatment period and achieved the smallest final tumor volume. In Figure 2(d), in accordance with the limitation of the daily radiation therapy dose, as expected, the maximum allowable daily dosage has been administered.

Among the 24 possible dynamical systems listed in Table 2, the four dynamical systems (13, 19, 20, and 21) with the lower costs have been selected.

Example 2. This example aims to compare results obtained from both direct and indirect methods. Here, the treatment strategy focuses on reducing tumor volume during treatment using the lowest possible anti-angiogenic and radiation agents as optimal regulator problem in Lagrange form. As in Example 1, we employ the four selected dynamical systems in order to make a regular comparison between two treatment strategies while serving the purpose of abbreviation. Other parameter values in performance index are given by $t_f = 10$, $\tau_p = 0$, $\theta_p = 1$, $\theta_u = 1$, and $\theta_w = 1$.

Figure 3 depicts the comparison of tumor volume, vascular carrying capacity, and the amounts of anti-angiogenic and radiation therapy for the four selected dynamical systems in Example 2. According to Figure 3(c), an anti-angiogenic drug is proposed with a bang-bang property for each selected dynamical system (13, 19, 20, and 21). Given the constraint on the daily permissible dose of radiation therapy within the acceptable range [58], it was as expected that the optimal radiation therapy dose would be selected as the highest possible value throughout the treatment (shown in Figures 2(d) and 3(d)).

5. Discussion of Results

Based on the numerical results reported in Section 4 regarding the dynamical system, solver method, and treatment strategy, we have arrived at the following findings.

5.1. Dynamical System.
Based on Example 1 and its numerical results, the discussion for the 24 distinct versions of a general dynamical system are as follows:

For stimulatory effect, one can say the following.

"By increasing α_s (which increases the tumor volume influence) or decreasing β_s (which decreases the carrying capacity influence), all values of J, $p(t_f)$, and $q(t_f)$ experience a significant decrease. This implies that if the stimulating effect of a tumor exceeds its volume in comparison to the vascular carrying capacity, there will be a substantial reduction in $p(t_f)$, $q(t_f)$, and the overall treatment cost. Consequently, low-cost treatments can be employed where tumor volume plays a crucial role in the stimulation effect."

For the inhibitory effect, we have the following.

"Through the α_i increase (which enhances the tumor volume influence) or the β_i decrease (which diminishes the carrying capacity impact), almost significant increases are observed in the values of J, $p(t_f)$, $q(t_f)$, and D_{AA}. This indicates that if the inhibitory effect of a tumor exceeds its volume in relation to the vascular carrying capacity, there will be substantial increases in tumor volume, vascular carrying capacity at the end of the treatment, and the overall treatment cost. Therefore, high-cost treatments can be justifiably applied where tumor volume plays a critical role in the inhibition effect.
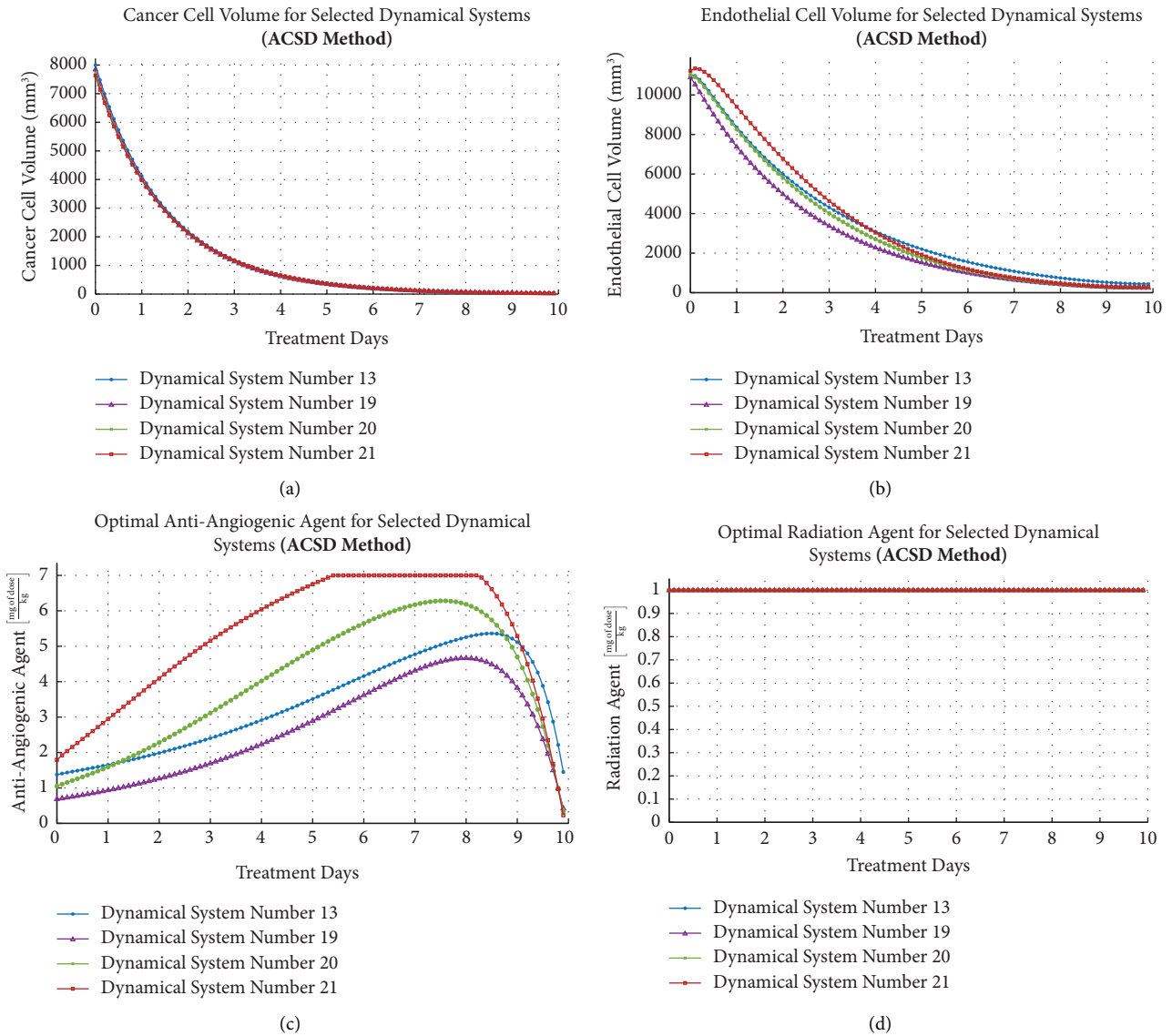
FIGURE 2: Optimal regulator problem in Bolza form: treatment strategy to reduce tumor volume at the final time based on data in Example 1 for the selected dynamical systems (13, 19, 20, and 21) using the Armijo conjugate steepest descent method. (a) Optimal cancer cell volume. (b) Optimal endothelial cell volume. (c) Optimal anti-angiogenic agent. (d) Optimal radiation agent.

For the dynamical systems, the following aspects can be considered.

"The Hahnfeldt dynamical system, among the four above selected dynamical systems, has consumed the highest amount of anti-angiogenic drugs. It can be concluded that the Hahnfeldt dynamical system compared to the three other dynamical systems (13, 19, and 20) has more resistance to treatment. Thus, in order to respond to the arguments in [40], we propose to the physician to use dynamical system number 19 that has less cost, tumor and carrying capacity volumes at final time, and total dose of anti-angiogenic agent among other dynamical systems."

5.2. Solver Method.
Considering the numerical results presented in Table 3 for the analysis of the solver methods, we have reached the following conclusions:

(i) In the Armijo conjugate steepest descent method, searching for the direction using the conjugate gradient method and determining the step length through the Armijo technique increase the execution time. However, the Armijo conjugate steepest descent solver is much faster than IPOPT-AMPL solver. On the other hand, the sequential quadratic Hamiltonian method is faster than the Armijo conjugate steepest descent method. Therefore, the Armijo conjugate steepest descent method takes the second place in terms of speed (see CPU time column in Table 3).

(ii) The execution speed of the IPOPT-AMPL method is very slow and depends on the lower bound values of state variables. If the lower bounds of the state variables are chosen to be greater than or equal to
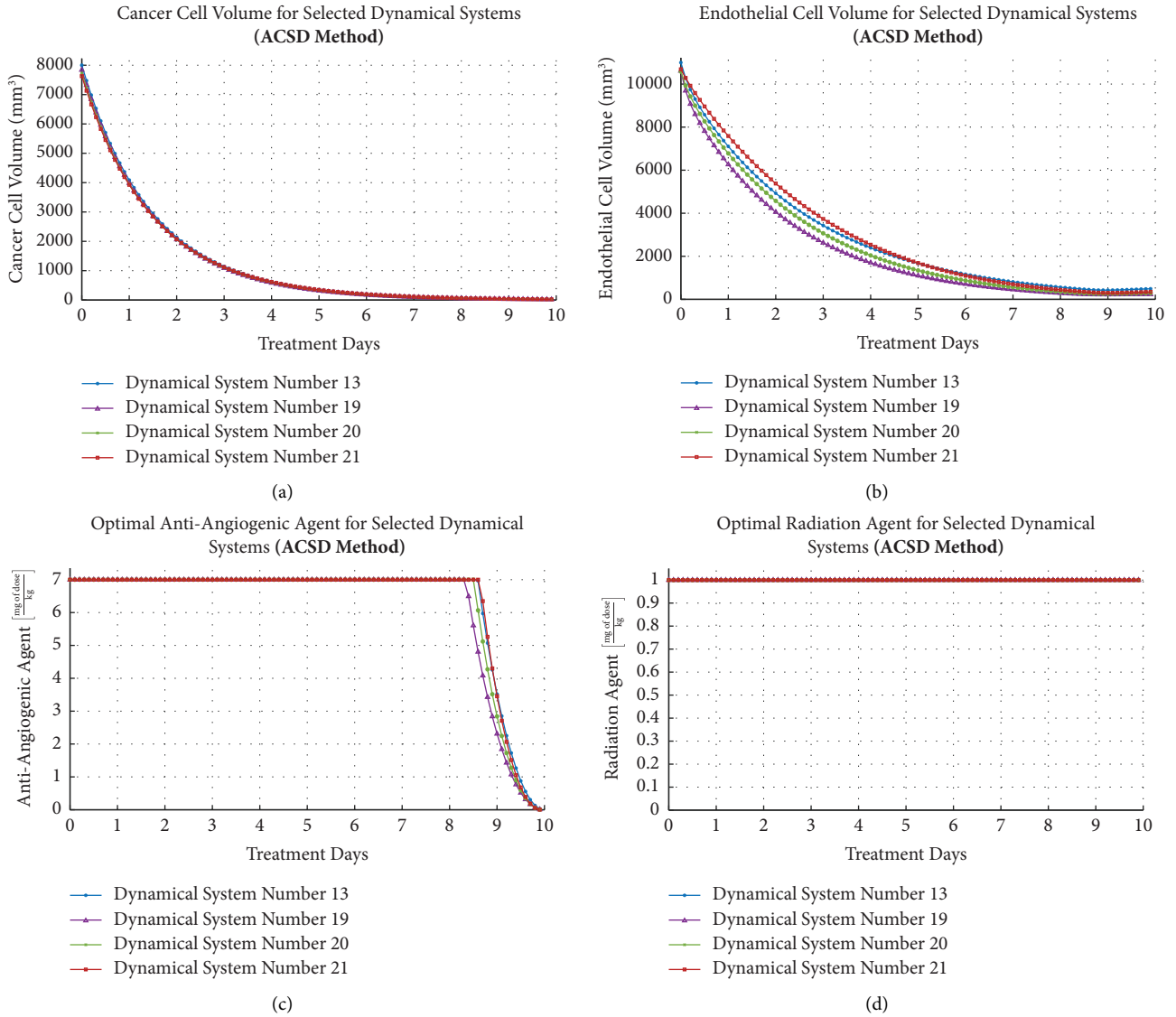
(a)

(b)

(c)

(d)

FIGURE 3: Optimal regulator problem in Lagrange form: treatment strategy to reduce tumor volume during 10 days treatment based on given values in Example 2 for the selected dynamical systems (13, 19, 20, and 21) using current ACSD method. (a) Optimal cancer cell volume. (b) Optimal endothelial cell volume. (c) Optimal anti-angiogenic agent. (d) Optimal radiation agent.

TABLE 3: Numerical results obtained by three different solvers (ACSD, SQH, and IPOPT-AMPL) applied to selected dynamical systems with a treatment strategy in Example 2.

No.	Solver	J^*	$p^*(t_f)$	$q^*(t_f)$	D^*_{AA}	D^*_{RA}	CPU time (s)
	ACSD	2.42252071×10^7	24.8355	491.3313	63.6117	10	4.4
13	SQH	2.42252072×10^7	24.8609	496.5655	63.4589	10	1.7
	IPOPT	2.42252099×10^7	24.6910	488.7144	63.7676	10	70
	ACSD	2.39545712×10^7	19.1978	235.3552	62.2380	10	6.4
19	SQH	2.39545712×10^7	19.1978	235.3557	62.2379	10	2.5
	IPOPT	2.39545728×10^7	19.0982	234.8001	62.2726	10	13.2
	ACSD	2.41563291×10^7	21.2859	295.4723	63.1083	10	5.9
20	SQH	2.41563291×10^7	21.2859	295.4725	63.1083	10	2.3
	IPOPT	2.41563311×10^7	21.1768	294.8252	63.1469	10	12
	ACSD	2.44238229×10^7	23.7813	351.1526	63.8398	10	7
21	SQH	2.44238229×10^7	23.7812	351.1491	63.8399	10	2.7
	IPOPT	2.44238254×10^7	23.6602	350.3479	63.8816	10	24.5

zero, then the IPOPT-AMPL encounters *"cannot compute 0/0"* error. This error is due to checking all grid points for the optimal value of NLP. Another disadvantage of the AMPL-IPOPT method is that it encounters a *"slack too small"* error when applied to dynamical systems 4, 5, 6, 11, and 12 with objective function in Example 2. Thus, there are limitations in the AMPL-IPOPT implementation, making it unsuitable for solving many optimal control problems, which has been confirmed and further analyzed in [59].

(iii) The Armijo conjugate steepest descent method almost provides a better solution for optimal control problems compared to the other two methods.

5.3. Treatment Strategy. Upon comparing the numerical results presented in Examples 1 and 2 to investigate the treatment strategies, one can conclude the following (see Tables 2 and 3).

"In the treatment strategy for reducing the cancer cell volume during treatment, a large amount of anti-angiogenic drug is used compared to the other treatment strategy. However, this strategy does not show a significant change in the reduction of tumor and vascular carrying capacity volumes. Additionally, the use of an anti-angiogenic drug with a bang-bang property contradicts the low-dose and continuous treatment approach for each of the selected dynamical systems (13, 19, 20, and 21) (see Figure 3(c)). Consequently, the administration of high doses of anti-angiogenic drug comes with its own side effects [60], which can be clinically harmful. However, if it is necessary to reduce the vascular carrying capacity volume, one can consider adopting the treatment strategy of decreasing tumor volume during treatment by using a higher dosage of anti-angiogenic drugs, while also accepting its associated side effects. By implementing this strategy, the probability of tumor growth after the treatment significantly decreases. On the other hand, for optimal control problems with dynamical system 19, the tumor volume at the final time reaches levels between 19 and 22, while the carrying capacity volume at the final time reaches levels between 235 and 240, indicating strong medical sense."

6. Conclusion

In this paper, cancer therapy with anti-angiogenic and radiotherapy treatments is discussed. The general dynamical system (15) is proposed. The hybrid indirect solver is proposed which successfully solves the related optimal control problems (33). Mathematically, the existence and uniqueness of the solution, as well as the convergence of the hybrid indirect method, were proven. The findings of this paper are as follows:

(a) The low-cost treatments can be employed, where tumor volume plays a crucial role in the stimulation effect.

(b) The application of high-cost treatments can be justified when tumor volume significantly influences the inhibitory effect.

(c) Offer to physicians and scientists: among the available options, there is at least one dynamical system that demonstrates lower costs, reduced tumor and carrying capacity volumes at the final time of treatment, and a lower total dose of the anti-angiogenic agent compared to the other dynamical systems.

(d) The Armijo conjugate steepest descent method almost offers a better solution for optimal control problems compared to the IPOPT-AMPL and SQH methods.

(e) Comparison of two treatment strategies (see Examples 1 and 2) makes it clear that the medical experts can use different strategies based on the situation and weights that they put on the way of the treatment.

In the next future work, we will mathematically present the reasons behind the resistance observed in reducing the carrying capacity of blood vessels when increasing the use of anti-angiogenic drugs.

Data Availability

No underlying data were collected or produced in this study.

Conflicts of Interest

The authors declare that there are no conflicts of interest regarding the publication of this article.

References

[1] F. Bray, M. Laversanne, E. Weiderpass, and I. Soerjomataram, "The ever-increasing importance of cancer as a leading cause of premature death worldwide," *Cancer*, vol. 127, no. 16, pp. 3029-3030, 2021.

[2] A. Malek and G. Abbasi, "Optimal control for Pennes' bioheat equation," *Asian Journal of Control*, vol. 18, no. 2, pp. 674–685, 2016.

[3] G. Abbasi and A. Malek, "Hyperthermia cancer therapy by domain decomposition methods using strongly continuous semigroups," *Mathematics and Computers in Simulation*, vol. 165, pp. 1–12, 2019.

[4] G. Abbasi and A. Malek, "Pointwise optimal control for cancer treatment by hyperthermia with thermal wave bioheat transfer," *Automatica*, vol. 111, Article ID 108579, 2020.

[5] M. E. Dastyar, A. Malek, S. Yousefi, and S. Yousefi, "Solving two-dimensional bioheat optimal control problem in solid and vessel domain by pseudospectral discretization," *Transactions of the Institute of Measurement and Control*, vol. 44, no. 12, pp. 2358–2368, 2022.

[6] G. Gasparini, R. Longo, M. Fanelli, and B. A. Teicher, "Combination of antiangiogenic therapy with other anticancer therapies: results, challenges, and open questions," *Journal of Clinical Oncology*, vol. 23, no. 6, pp. 1295–1311, 2005.

[7] P. Hahnfeldt, D. Panigrahy, J. Folkman, and L. Hlatky, "Tumor development under angiogenic signaling: a dynamical theory of tumor growth, treatment response, and post-vascular dormancy," *Cancer Research*, vol. 59, no. 19, pp. 4770–4775, 1999.

[8] A. Ergun, C. Kevin, and L. M. Wein, "Optimal scheduling of radiotherapy and angiogenic inhibitors," *Bulletin of Mathematical Biology*, vol. 65, no. 3, pp. 407–424, 2003.

[9] H. Schättler and U. Ledzewicz, "Optimal control for mathematical models of cancer therapies," *An application of geometric methods*, Springer, Berlin, Germany, 2015.

[10] G. Kienle, L. Melina, B. Tim, C. Kurt, and A. Borzì, "Modeling and numerical solution of a cancer therapy optimal control problem," *Applied Mathematics*, vol. 9, no. 8, 2018.

[11] K. M. Owolabi, K. C. Patidar, and A. Shikongo, "Numerical solution for a problem arising in angiogenic signalling," *AIMS Mathematics*, vol. 4, no. 1, pp. 43–60, 2019.

[12] M. Athans and L. Peter, *Falb. Optimal Control: An Introduction to the Theory and its Applications*, Courier Corporation, North Chelmsford, MA, USA, 2013.

[13] D. A. Benson, G. T. Huntington, and T. P. Thorvaldsen, "Direct trajectory optimization and costate estimation via an orthogonal collocation method," *Journal of Guidance, Control, and Dynamics*, vol. 29, no. 6, pp. 1435–1440, 2006.

[14] D. G. Hull, *Optimal Control Theory for Applications*, Springer Science Business Media, Berlin, Germany, 2013.

[15] J. Jahn, *Introduction to the Theory of Nonlinear Optimization*, Springer Nature, Berlin, Germany, 2020.

[16] D. P. Bertsekas, "Nonlinear programming," *Journal of the Operational Research Society*, vol. 48, no. 3, p. 334, 1997.

[17] A. V. Rao, "A survey of numerical methods for optimal control," *Advances in the Astronautical Sciences*, vol. 135, no. 1, pp. 497–528, 2009.

[18] S. S. Rao, *Engineering Optimization: Theory and Practice*, John Wiley Sons, Hoboken, NJ, USA, 2019.

[19] T. J. Böhme, B. Frank, T. J. Böhme, and B. Frank, "Direct methods for optimal control," *Hybrid systems, optimal control and hybrid vehicles: Theory, methods and applications*, Springer, Berlin, Germany, 2017.

[20] K. M. C. Tjørve, E. Tjørve, and E. Tjørve, "The use of Gompertz models in growth analyses, and new Gompertz-model approach: an addition to the Unified-Richards family," *PLoS One*, vol. 12, Article ID e0178691, 6 pages, 2017.

[21] C. Vaghi, A. Rodallec, R. Fanciullino et al., "Population modeling of tumor growth curves and the reduced Gompertz model improve prediction of the age of experimental tumors," *PLoS Computational Biology*, vol. 16, no. 2, Article ID e1007178, 2020.

[22] B. Ribba, N. H. Holford, P. Magni, and I. Trocóniz, "A review of mixed-effects models of tumor growth and effects of anticancer drug treatment used in population analysis," *CPT: Pharmacometrics & Systems Pharmacology*, vol. 3, no. 5, pp. 113–210, 2014.

[23] J. Cohen, P. Cohen, S. G. West, and L. S. Aiken, *Applied Multiple Regression/correlation Analysis for the Behavioral Sciences*, Routledge, Oxfordshire, UK, 2013.

[24] L. Norton and R. Simon, "Growth curve of an experimental solid tumor following radiotherapy," *Journal of the National Cancer Institute: Journal of the National Cancer Institute*, vol. 58, no. 6, pp. 1735–1741, 1977.

[25] L. Norton, "A Gompertzian model of human breast cancer growth," *Cancer Research*, vol. 48, no. 1, pp. 7067–7071, 1988.

[26] H. L. Royden and P. Fitzpatrick, *Real Analysis*, vol. 2, Macmillan, New York, NY, USA, 1968.

[27] E. D. Sontag and S. P. Boyd, "Mathematical control theory: deterministic finite-dimensional systems," *IEEE Transactions on Automatic Control*, vol. 40, no. 3, p. 563, 1995.

[28] A. M. E. Abdalla, L. Xiao, M. W. Ullah, M. Yu, C. Ouyang, and G. Yang, "Current challenges of cancer anti-angiogenic therapy and the promise of nanotherapeutics," *Theranostics*, vol. 8, no. 2, pp. 533–548, 2018.

[29] V. Aydogan, *Understanding endothelial cell behaviors during sprouting angiogenesis*, Ph.D. Dissertation, University of Basel, Basel, Switzerland, 2016.

[30] Z.-L. Liu, H.-H. Chen, L. Zheng, L. P. Sun, and L. Shi, "Angiogenic signaling pathways and anti-angiogenic therapy for cancer," *Signal Transduction and Targeted Therapy*, vol. 8, no. 1, p. 198, 2023.

[31] N.. Ferrara, "Vascular endothelial growth factor: basic science and clinical progress," *Endocrine Reviews*, vol. 25, no. 4, pp. 581–611, 2004.

[32] L. Claesson-Welsh and M. Welsh, "VEGFA and tumour angiogenesis," *Journal of Internal Medicine*, vol. 273, no. 2, pp. 114–127, 2013.

[33] X. Li and U. Eriksson, "Novel vegf family members: vegf-b, vegf-c and vegf-d," *The International Journal of Biochemistry & Cell Biology*, vol. 33, no. 4, pp. 421–426, 2001.

[34] M. R. Mancuso, R. Davis, S. M. Norberg, S. O'Brien, B. Sennino, and T. Nakahara, "Rapid vascular regrowth in tumors after reversal of VEGF inhibition," *Journal of Clinical Investigation*, vol. 116, no. 10, pp. 2610–2621, 2006.

[35] J. M. L. Ebos and R. S. Kerbel, "Antiangiogenic therapy: impact on invasion, disease progression, and metastasis," *Nature Reviews Clinical Oncology*, vol. 8, no. 4, pp. 210–221, 2011.

[36] J. M. L. Ebos, C. R. Lee, W. Cruz-Munoz, G. A. Bjarnason, and J. G. Christensen, "Accelerated metastasis after short-term treatment with a potent inhibitor of tumor angiogenesis," *Cancer Cell*, vol. 15, no. 3, pp. 232–239, 2009.

[37] C. E. Round, M. V. Williams, T. Mee et al., "Radiotherapy demand and activity in England 2006–2020," *Clinical Oncology*, vol. 25, no. 9, pp. 522–530, 2013.

[38] F. Forouzannia, H. Enderling, and M. Kohandel, "Mathematical modeling of the effects of tumor heterogeneity on the efficiency of radiation treatment schedule," *Bulletin of Mathematical Biology*, vol. 80, no. 2, pp. 283–293, 2018.

[39] L. M. Wein, J. E. Cohen, and J. T. Wu, "Dynamic optimization of a linear–quadratic model with incomplete repair and volume-dependent sensitivity and repopulation," *International Journal of Radiation Oncology, Biology, Physics*, vol. 47, no. 4, pp. 1073–1083, 2000.

[40] U. Ledzewicz and H. Schättler, "Multi-input optimal control problems for combined tumor anti-angiogenic and radiotherapy treatments," *Journal of Optimization Theory and Applications*, vol. 153, no. 1, pp. 195–224, 2012.

[41] D. Draganov, S. Gopalakrishna-Pillai, Y.-R. Chen et al., "Modulation of P2X 4/P2 X7/Pannexin-1 sensitivity to extracellular ATP via Ivermectin induces a non-apoptotic and inflammatory form of cancer cell death," *Scientific Reports*, vol. 5, no. 1, Article ID 16222, 2015.

[42] A. López-Jiménez, M. García-Caballero, M. Á. Medina, and A. R. Quesada, "Anti-angiogenic properties of carnosol and carnosic acid, two major dietary compounds from rosemary," *European Journal of Nutrition*, vol. 52, no. 1, pp. 85–95, 2013.

[43] L. Barazzuol, R. P. Coppes, and P. van Luijk, "Prevention and treatment of radiotherapy-induced side effects," *Molecular Oncology*, vol. 14, no. 7, pp. 1538–1554, 2020.

[44] J. Nocedal and S. J. Wright, *Numerical Optimization*, Springer, Berlin, Germany, 1999.

[45] L. Urszula and H. Schättler, "Antiangiogenic therapy in cancer treatment as an optimal control problem," *SIAM Journal on Control and Optimization*, vol. 46, no. 3, pp. 1052–1079, 2007.

[46] P. N. Paraskevopoulos, *Modern Control Engineering*, CRC Press, Boca Raton, FL, USA, 2017.

[47] J. T. Betts, *Practical methods for optimal control and estimation using nonlinear programming*, Society for Industrial and Applied Mathematics, Philadelphia, PA, USA, 2010.

[48] D. E. Kirk, *Optimal Control Theory: An Introduction*, Courier Corporation, North Chelmsford, MA, USA, 2004.

[49] K. Chudej, L. Wagner, and H. J. Pesch, "Numerical solution of an optimal control problem in cancer treatment: combined radio and anti-angiogenic therapy," *IFAC-PapersOnLine*, vol. 48, no. 1, pp. 665-666, 2015.

[50] U. Ledzewicz, H. Maurer, and H. Schättler, "Optimal combined radio-and anti-angiogenic cancer therapy," *Journal of Optimization Theory and Applications*, vol. 180, no. 1, pp. 321–340, 2019.

[51] A.. Wachter, *An interior point algorithm for large-scale nonlinear optimization with applications in process engineering*, Ph.D. Dissertation, Carnegie Mellon University, Pittsburgh, PA, USA, 2002.

[52] A. Wächter and L. T. Biegler, "On the implementation of an interior-point filter line-search algorithm for large-scale nonlinear programming," *Mathematical Programming*, vol. 106, no. 1, pp. 25–57, 2006.

[53] R. Fourer, D. M. Gay, and B. W. Kernighan, *AMPL A Modeling Language for Mathematical Programming*, Princeton University, Princeton, NJ, USA, 2003.

[54] I. A. Krylov, "An algorithm for the method of successive approximations in optimal control problems," *USSR Computational Mathematics and Mathematical Physics*, vol. 12, no. 1, pp. 15–38, 1972.

[55] R. Fletcher, *Practical Methods of Optimization*, John Wiley Sons, Hoboken, NJ, USA, 2013.

[56] L. Armijo, "Minimization of functions having Lipschitz continuous first partial derivatives," *Pacific Journal of Mathematics*, vol. 16, no. 1, pp. 1–3, 1966.

[57] G. Zoutendijk, "Nonlinear programming, computational methods," *Integer and nonlinear programming*, vol. 1, pp. 37–86, 1970.

[58] R. S. A. Goedegebuure, L. K. De Klerk, A. J. Bass, S. Derks, and V. L. J. L. Thijssen, "Combining radiotherapy with anti-angiogenic therapy and immunotherapy; a therapeutic triad for cancer?" *Frontiers in Immunology*, vol. 9, p. 3107, 2018.

[59] H. Pirnay, R. López-Negrete, and L. T. Biegler, "Optimal sensitivity based on IPOPT," *Mathematical Programming Computation*, vol. 4, pp. 307–331, 2012.

[60] F. Elice and F. Rodeghiero, "Side effects of anti-angiogenic drugs," *Thrombosis Research*, vol. 129, pp. S50–S53, 2012.